Evaluation of the Forward Scattering Spectrometer Probe. Part III: Time Response and Laser Inhomogeneity Limitations

DARREL BAUMGARDNER AND MICHAEL SPOWART

National Center for Atmospheric Research, Boulder, Colorado*

(Manuscript received 8 September 1989, in final form 23 March 1990)

ABSTRACT

The electronic response time of the Forward Scattering Spectrometer Probe (FSSP) has been evaluated and is shown to affect the measurement of droplet size. The size of droplets are underestimated when airspeeds exceed 50 m s^{-1} and size distributions are broadened as a result of nonuniformities in the laser beam of the probe.

A processing scheme that requires a detailed knowledge of a probe's optical and electronic characteristics is described that compensates for the measurement errors caused by the probe's electronic and optical limitations.

1. Introduction

The PMS (Particle Measuring Systems, Inc., Boulder, Co.) FSSP is a widely used instrument for the measurement of droplet size distributions. This probe has found extensive use in studies of cloud microphysical processes, aircraft icing, spray characteristics, and other areas of research that require detailed information about the size and concentration of droplets and the temporal and spatial evolution of these droplet distributions.

The operating characteristics and measurement limitations have been evaluated extensively. Pinnick (1981) studied the effects of changes in droplet index of refraction and scattering angles on measurements from the FSSP. He showed that the optical response can be adequately modeled by Mie theory, but that the size channel widths in the probe must be adjusted to minimize ambiguities in size measurements. Baumgardner (1983) evaluated a number of droplet and liquid water measuring instruments, estimated their measurement uncertainties, and compared their responses during in-cloud measurements. His studies showed that large concentration errors will result when auxiliary information from the FSSP is not used to properly define the sample volume. Cerni (1983) showed that the FSSP size calibration must be adjusted to properly fit the Mie scattering curve and was also the first to discuss the undersizing of droplets at airspeeds greater than 55 m s^{-1}. Both Baumgardner and Cerni recognized the artificial broadening of the size distribution caused by the FSSP but did not identify the source of this effect or the magnitude of the spreading. Dye and Baumgardner (1984) evaluated the optical and electronic characteristics of a number of FSSPs and illustrated the importance of knowing the operating characteristics of individual probes since major differences existed among the probes they evaluated. Baumgardner et al (1985) further evaluated the effects of electronic deadtime and optical coincidence and developed algorithms that compensated for these effects. However, Cooper (1988) has shown that the coincidence corrections depend not only upon the magnitude of the total concentration, but also on the relative shape of the size distribution and the optical and electronic characteristics of each probe. More recently, Brengier (1989a,b) has derived an alternative method for correcting coincidence and deadtime losses and has also demonstrated that the activity measurement is a good indicator of small scale inhomogeneities in the cloud structure.

As a result of these studies, the functioning of the FSSP is much better understood, and the quality of measurements improved. However, significant discrepancies are observed sometimes in comparisons between measurements from the FSSP and other droplet measurement instruments. A number of cloud droplet probes owned by the National Center for Atmospheric research were flown on the University of Wyoming Beechcraft Kingair during the 1985 Joint Hawaiian Warm Rain Project (JHWRP). In addition to an FSSP, a PMS one-dimensional optical array probe (a 260× with 10 μm size resolution) was used to measure in the size range from 40–150 μm. The 1D probe has response time limitations that affect the sample volume

* The National Center for Atmospheric Research is sponsored by the National Science Foundation.

Corresponding author address: Dr. Darrel Baumgardner, NCAR, P.O. Box 3000, Boulder, Colorado 80307-3000.

(Baumgardner 1987) and limits the smallest detectable size to about 40 μm at the typical research airspeeds (about 80–100 m s^{-1}). However, corrections minimize these measurement errors. Figure 1 illustrates an average of a number of measurements from both of these instruments. The overlap region between the two probes is relatively narrow; however, in general, the transition in this region should be smooth. The discontinuity indicates a possible problem with the FSSP data, at least with respect to the 260X measurements.

The NCAR FSSP used in the JHWRP was carefully calibrated and maintained throughout the project. Calibration with glass beads showed that the FSSP was apparently sizing according to the manufacturer specifications. All corrections suggested by earlier studies were applied to the measurements shown in Fig. 1. As a result of the persistent discrepancy between the measurements from the two instruments, a further evaluation of the operating characteristics of the FSSP was conducted to investigate other possible causes for measurement differences. These investigations focused on factors that might affect the performance of the probe when operated in normal research conditions but would not be evident in laboratory tests and calibrations.

A number of possibilities were evaluated and the electronic response time of the probe and laser intensity inhomogeneities seem to have the most significant effect on the FSSP measurements. The remainder of this paper discusses the nature and the magnitude of these error sources and describes a technique by which their effect on the measurements may be compensated.

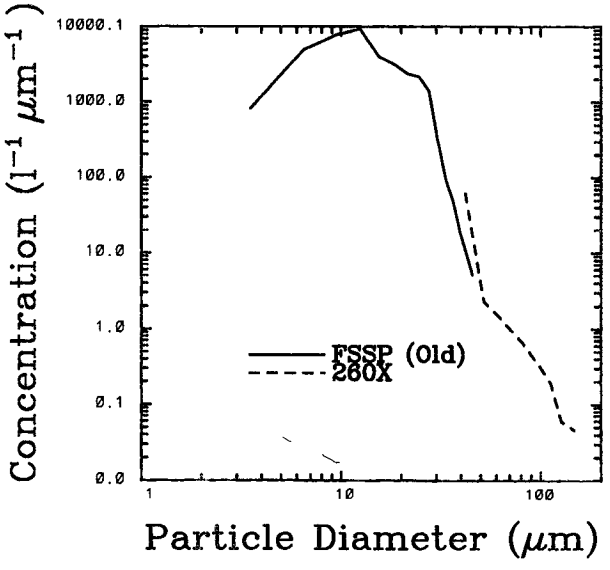

FIG. 1. The FSSP and 260X measurements averaged over several cloud passes are compared in this figure. The FSSP sample volume and size calibration are nominal manufacturer values.

2. Response time limitations

The FSSP's principles of operation have been described extensively (e.g. Knollenberg 1981; Dye and Baumgardner 1984). However, a brief summary of the components of operation pertinent to the topic of this paper is in order.

The FSSP detects droplets passing through a laser beam by measuring the scattered light that is collected through a solid angle defined by the optical geometry. The relationship between droplet size and measured light intensity has been determined from Mie scattering theory, assuming certain droplet shape and composition properties. The peak signal is converted to a droplet size using a 15-channel pulse–height analyzer (PHA) whose comparator levels are preset to correspond to specific size intervals. The instrument is calibrated using monodispersed glass beads of known size and index of refraction.

a. Circuit response time

The light scattered by a droplet is converted to an electrical current by a photodetector and then conditioned through a number of stages before reaching the pulse–height analyzer. The response characteristics of each of the signal conditioning stages is a function of the bandwidth of the operational amplifiers and the respective values of the passive components that are selected to stabilize the circuits. It is possible to develop an analytical description of the analog circuit and from this to estimate the response to impulses caused by droplets scattering light into the optics. However, a simpler, empirical solution is to measure the response of the circuit directly and find a function that sufficiently models this response.

This alternative approach was selected and the circuit response was measured by attaching the photodetector to a red, light-emitting diode (LED) that had a rise time shorter than 40 ns. This LED was activated with a pulse train generated by a function generator. Both the pulse width and frequency were independently controlled. The amplitude of the signal at the pulse height analyzer was measured as a function of the input pulse width, t, and amplitude, V_i. An exponential function of the form

$$v_o = V_i(1.0 - e^{-t/\tau}) \tag{1}$$

was found to approximate the response, where τ is the response time of the circuit. The pulse width is related to the velocity, v, of droplets through the beam by the relation

$$t = \frac{d}{v} \tag{2}$$

where d is the chord length through which droplets pass when penetrating the beam. This function is shown compared with the measured response in Fig. 2 for the

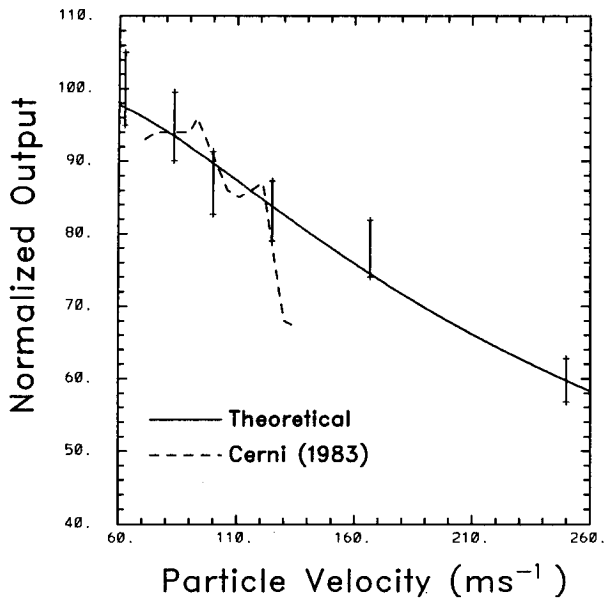

FIG. 2. The measured, normalized voltage at the input to the pulse height analyzer is shown here as a function of particle airspeed, computed as the product of the pulsewidth, t, of the pulsed LED and an assumed beam diameter of 0.2 mm. The length of the bars represent the measurement uncertainty and the solid continuous line is the function, $1.0 - \exp(-t/\tau)$, where τ is the measured electronic risetime = 0.55 μs. The results of Cerni (1983) are plotted as an independent comparison.

FSSP used in the JHWRP. The response time, τ, is 0.55 μs for this probe, but for other probes has been measured over a range between 0.4 and 0.7 μs. The results of Cerni (1983) have been transformed to similar coordinates and plotted on the figure for the purpose of comparison. The FSSP used in his studies quite possibly had a different response time than the probe evaluated in the present study. However, the response of Cerni's study is in relatively good agreement.

b. Response time effects on droplet sizing

Equation (1) predicts the response of the FSSP's circuit for the event of a droplet entering the beam when it is taken as a step function, i.e. no scattered light when the droplet is outside the beam and a constant value the instant the droplet enters the beam. This assumes that the droplet diameter is much smaller than the diameter of the laser and that the intensity distribution over the laser beam's cross section is uniform.

The multimode laser used in the FSSP was selected to produce a high probability of a droplet passing through a peak intensity regardless of where it passes through the beam. The photograph shown in Fig. 3 is of the expanded beam of the JHWRP FSSP laser and illustrates the inhomogeneities in the intensity distribution. The intensity was measured by removing the right-angle mirror in the transmitting arm of the FSSP before projecting the beam onto a photodetector. This photodetector was moved with a micropositioner to measure the light intensity as a function of distance from the edges of the beam. Figure 4 shows an intensity map derived from these measurements. Each contour represents the fraction of the maximum light intensity measured in the beam. Additional measurement has been made of three other FSSP lasers with similar results. This intensity distribution invalidates the assumption necessary to use (1) as a model of the probe's electronic response. However, (1) can still be used if the incident light is approximated as a series of step inputs whose values are determined from the measured intensity pattern. With this approximation, (1) is applied with different boundary conditions at each new change in intensity.

The intensity distribution shown in Fig. 4 indicates that the intensity of light scattered by a droplet will depend upon where it passes through the beam. Accordingly, the response of the FSSP to a droplet is characterized by a range of values calculated by evaluating (1) in discrete steps as the droplet proceeds along a particular path. The solution to (1) for the measured amplitude at each location in the beam is

$$v(t_i) = v(t_{i-1}) + C(1 - e^{-(t_i - t_{i-1})/\tau}) \qquad (3)$$

$$C = V_i - v(t_{i-1})$$

where

V_i Amplitude of the beam at the ith grid point
t_i Elapsed time at the ith grid point since first penetration of the beam.

Figure 5 shows the estimated droplet size as a function of actual size for an airspeed of 80 m s^{-1}, typical for the Hawaiian project. The intensity inhomogeneities of the laser beam also contribute to the spreading

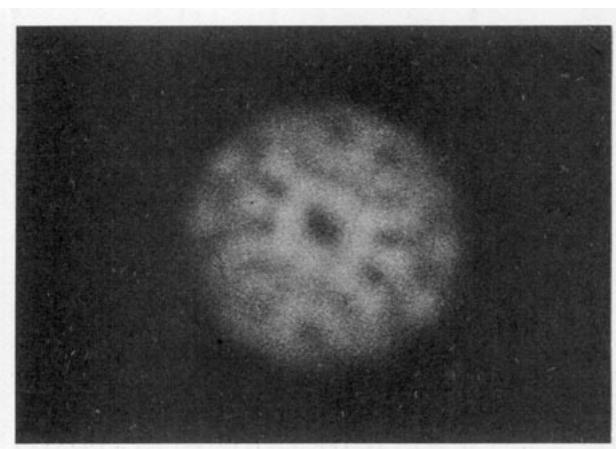

FIG. 3. This photograph shows the beam intensity pattern of a multimode laser used in an FSSP.

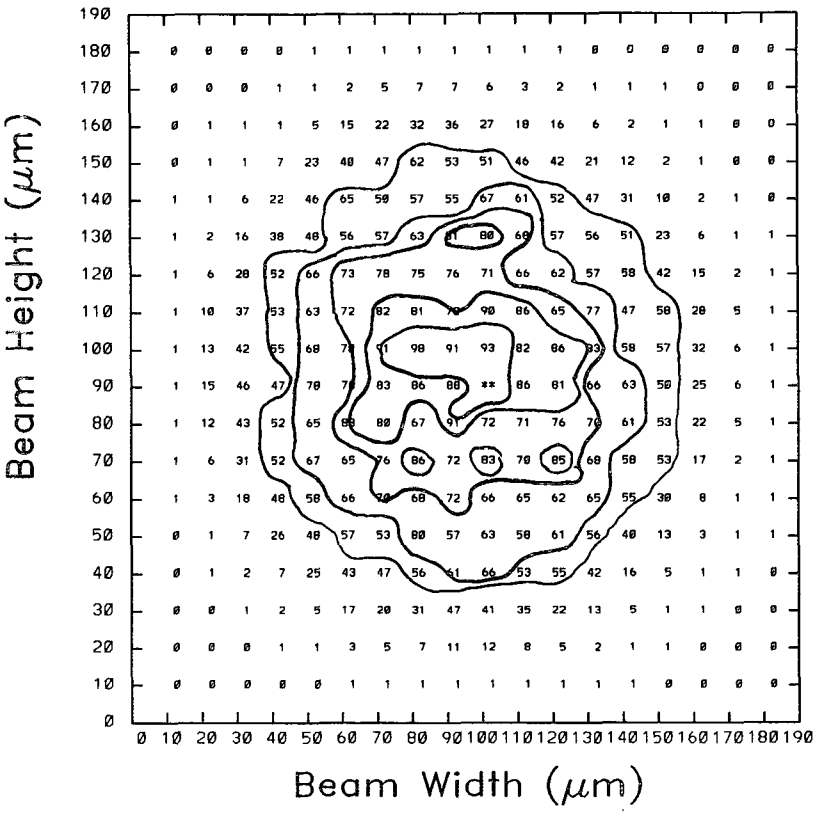

FIG. 4. The contour map presented in this figure illustrates the measured intensity values across the laser beam shown in Fig. 3. The values shown are percentages of the maximum value measured (**). The contours are 50–90% in 10% steps.

of the actual size distribution. In Fig. 5 the vertical bars at each data point correspond to the minimum and maximum values found for each of 20 different droplet paths where the distance between paths was 10 μm. The contour map, shown in Fig. 4, shows that the maximum intensity of this particular laser is in a relatively small section of the beam near its center. The majority of droplets will pass through sections of the beam where the peak intensity is 80%–90% of the maximum. The measured size distribution will be broader than the actual distribution as a result of the intensity variation and the additional effect of the electronic response time. This spreading can be illustrated by FSSP measurements of glass beads whose sizes have been determined from microphotographs. Beads with a water equivalent size of 22 μm were drawn through the FSSP at a relatively low rate (15 m s^{-1}). These beads should appear in the size channels of the FSSP shown by the solid line in Fig. 6 if there was no instrumental broadening. The dashed line, which is the measured size distribution, shows a response much broader than expected. This spreading was modeled with (3) by using the glass bead distribution as the input and then calculating an estimate of the measured sizes as the beads pass through different chords of the laser beam whose intensity profile is shown in Fig. 4. If the true size is assumed to be measured when the droplets pass through the average beam intensity, then the droplet will be oversized when passing through the center of the beam and undersized while passing further away from the center. The size distribution drawn as a dotted line in Fig. 6 represents the result of this simulation. The measured and estimated distributions show similar characteristics; however, the measured distribution shows more counts in larger sizes and the simulated distribution has more in the smaller sizes. Coincidence of beads in the beam will cause the oversizing seen in the larger size channels of the measured distribution (Cooper 1988). The simulated distribution assumes that droplets along a particular chord are illuminated only at the intensity that was measured for that particular path. However, in reality, the light varies in a nondiscrete fashion and the intensity of light illuminating a droplet is composed of a field of intensities, varying about the discrete value that was measured in the mapping procedure. Thus, the simulation probably overestimates the degree of undersizing. However, the general behavior of the simulation demonstrates that

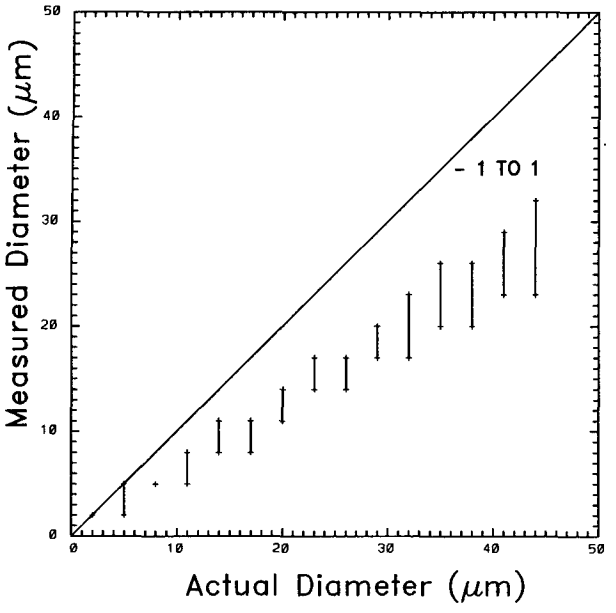

FIG. 5. The measured and actual droplet sizes are compared in this figure. The measured droplet size takes into account the effects of time response and beam intensity nonuniformities. The vertical bars represent the range of values possible as the droplet passes through different parts of the beam.

beam intensity inhomogeneities are most likely the major cause for instrumental broadening of the size distribution.

The undersizing and spreading of the distribution can be partially compensated if the response time of the electronics and intensity distribution of the laser is known. Details of these corrections are discussed in the next section.

d. Method of correction

The response characteristics of the FSSP can be appropriately modeled using the measured electronic response time and laser intensity cross section for a specific probe. This model is then used to derive an estimate of the real droplet distribution from that which is measured. The algorithm for deriving this estimate takes the form

$$\mathbf{S}_M = \mathbf{A}\mathbf{S}_T \tag{4}$$

where $\mathbf{S}_M$ is a 15×1 matrix of the measured counts in each of the fifteen size channels and $\mathbf{A}$ is the 15×15 matrix that characterizes the response of a particular instrument. The 15×1 matrix $\mathbf{S}_T$ is the true droplet distribution. The A_{ij}th element of $\mathbf{A}$ represents the fraction of droplets measured in size class i that come from the actual size class j. For example, the elements in column j of this matrix are determined by evaluating (4) for a droplet of size class i as it passes through each path of the mapped laser beam. These paths may result in measured sizes larger, smaller, and the same as the selected size class. The fraction of passes that cause a droplet of size j to be measured becomes the ijth element of the response matrix.

The procedure for solving (4) for a given true airspeed and beam fraction (that portion that is defined by the velocity acceptance test) is as follows.

1) For each true size j: for each beam position k, calculate measured channel $M(j, k)$, calculate acceptance matrix $\mathbf{d}(j, k)$; $\mathbf{d}(j, k) = 0$, if k outside beam fraction, $\mathbf{d}(j, k) = 1$, if k inside beam fraction.

2) Calculate the response matrix $\mathbf{A}$

$$A(i, j) = \frac{1}{n} \sum_{k=1}^{n} \delta(M(j, k), i)\mathbf{d}(j, k) \tag{5}$$

where δ is the usual Kronecker delta function and n is the total number of mapped beam paths.

3) If possible, compute $\mathbf{A}^{-1}$ and solve (4) directly to obtain $\mathbf{S}_T$. Otherwise, proceed with steps 4–7. This latter event is a common occurrence since the response matrix is often singular and can not be inverted.

4) Make an initial guess of $\mathbf{S}_T$.

5) Evaluate (4) to obtain an estimate $\mathbf{S}'_M$.

6) Calculate the error matrix $\mathbf{S}_M - \mathbf{S}'_M$.

7) If the error is greater than some preselected value, make a new guess of $\mathbf{S}_T$ and repeat steps 5–7.

A number of techniques have been developed for solving this particular inversion problem (e.g. Wolfe 1959; Markowski 1987) and a solution can usually be found after only a few iterations.

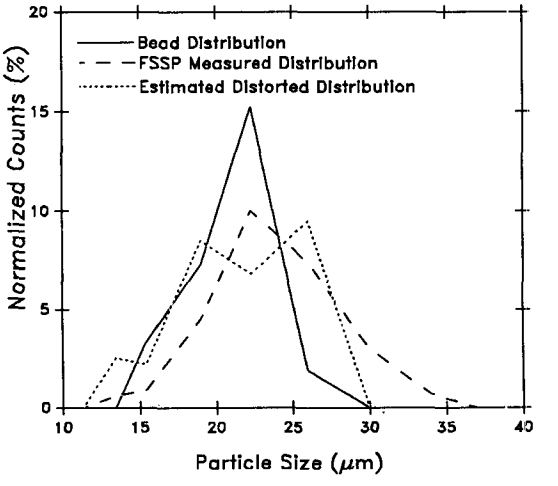

FIG. 6. The effect of the inhomogeneous beam intensity is demonstrated here with normalized distributions of glass bead calibration particles (solid line), the distribution measured with the FSSP (dashed), and the predicted FSSP response (dotted).

3. Discussion

The response characteristics of the FSSP distort actual size distributions and, in some cases, the inversion technique can only partially correct for these distortions. Figures 7a–c demonstrate several aspects of the problem. In these figures the distribution shown with the solid line indicates a hypothetical size spectrum, the histogram drawn with dots is created by multiplying the hypothetical matrix of counts by the response matrix, and the dashed line is the result of applying a correction algorithm to this matrix of "measured" counts. The correction algorithm implemented is the technique of Markowski (1987). All calculations were made using the measured intensity distribution shown in Fig. 4, a beam diameter of 0.2 mm, a response time of 0.6 μs, and an airspeed of 100 m s^{-1}.

Figure 7a illustrates the expected response to a size distribution that is uniformly constant over all size ranges of the FSSP, and no droplets larger than the highest size channel. The measured distribution shows no counts in the upper two size channels because they have been undersized into smaller channels. Similarly, droplets with first and second channel sizes are undersized such that they do not reach the minimum size limit of the probe and the counts occurring in these channels are from larger droplets that were undersized. The correction is unable to produce the original distribution because not enough information is available about the concentration of droplets outside the range of the probe and the result is an overestimate of counts in the mid-size ranges and an underestimate in the end channels. Figures 7b and 7c illustrate the response of the probe to monodispersed and unimodal distributions, respectively. In these cases the measured distribution is shifted to smaller sizes and broadened. The reconstructed distributions are nearly the same as the original and would have converged to the same value

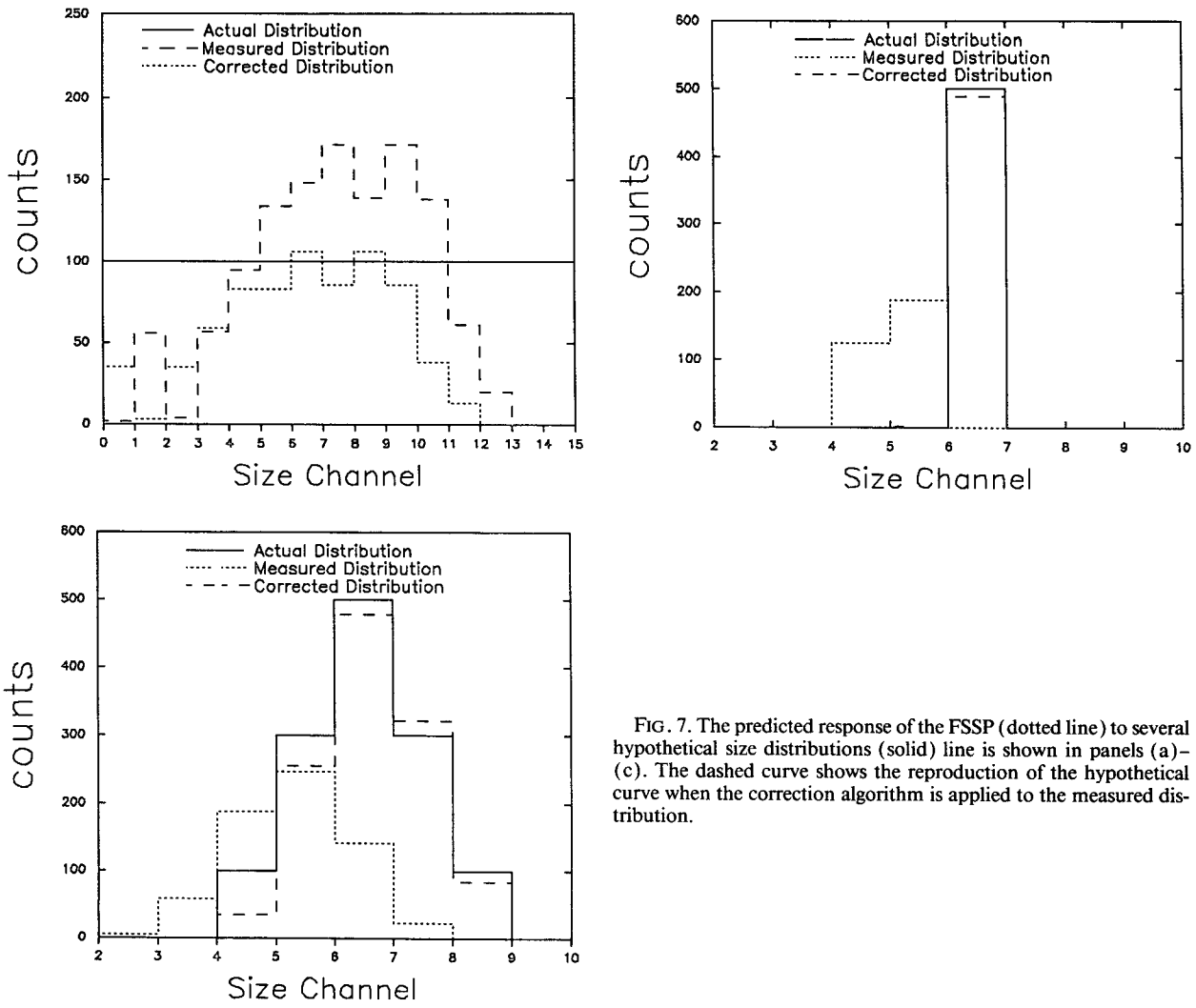

FIG. 7. The predicted response of the FSSP (dotted line) to several hypothetical size distributions (solid) line is shown in panels (a)–(c). The dashed curve shows the reproduction of the hypothetical curve when the correction algorithm is applied to the measured distribution.

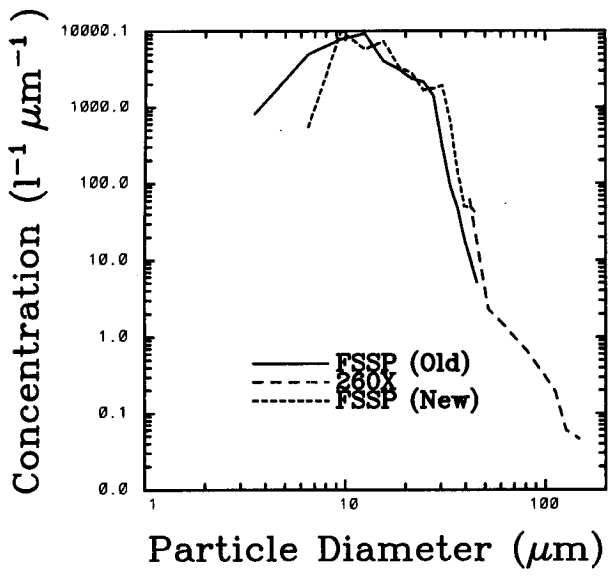

FIG. 8. This figure is a duplicate of Fig. 1 but with the addition of the corrected FSSP measurements.

if the error limit specified in the algorithm would have been set to a smaller value.

The FSSP measurements shown in Fig. 1 were corrected with the Markowski algorithm and comparisons with the measurements of the OAP-260X droplet distributions are shown in Fig. 8. The comparison of size distributions from the two instruments in the overlap region shows a much closer agreement after corrections are applied.

This evaluation has demonstrated the effect that the electronic time response and inhomogeneous beam intensity has on the FSSP measurements. Corrections can be made to the measurements that partially correct the missizing caused by these response characteristics of the probe. The rise time of the FSSP electronics must be measured and the intensity distribution of the laser beam mapped before these corrections can be applied. Measurements of the laser intensity have not been made at different cross sections of the beam within the depth-of-field. However, the intensity variations seem to originate within the laser tube and are not expected to vary along the beam within the sample volume.

The measurement response of the FSSP would be significantly improved by replacing the amplifiers presently used in the FSSP with more modern, high frequency components that improve the instrument's frequency response to at least 10 mHz. This improvement is necessary if the probe is to be used effectively on higher altitude, high-speed aircraft such as used by many research organizations. The problem of spectral broadening caused by the intensity inhomogeneities is more difficult to solve since there are no lasers available with sufficiently uniform, homogeneous distributions. A possible solution is to use a laser with a better defined intensity profile, e.g. a Gaussian mode laser. This would not alleviate the problem but would make the response matrix calculation simpler and more uniform from probe to probe. This possibility is presently being explored for future modifications to the FSSP.

The evaluation of this study was focused on a particular FSSP. However, measurements of four other probes show similar optical and electronic characteristics. The results of this study should be applicable to other FSSPs once their optical and electronic properties have been adequately characterized.

Acknowledgments. The authors would like to thank the Research Aviation Facility for its support, Bill Dawson for his assistance in making the necessary electronic response measurements, and the University of Wyoming, whose aircraft was used during the Joint Hawaiian Warm Rain Project. Our appreciation is also extended to W. A. Cooper and J. E. Dye for their careful reviews of this manuscript.

REFERENCES

Baumgardner, D., 1983: An analysis and comparison of five water droplet measuring instruments. *J. Appl. Meteor.*, **22**, 891–910.

——, 1987: Corrections for the response times of particle measuring probes. Preprints, *Sixth Symp. on Meteorological Observations and Instrumentation*, New Orleans, Amer. Meteor. Soc., 148–151.

——, W. Strapp and J. E. Dye, 1985: Evaluation of the Forward Scattering Spectrometer Probe. Part II: Corrections for coincidence and dead-time losses. *J. Atmos. Oceanic Technol.*, **2**, 626–632.

Brengier, J. L., 1989: Coincidence and dead-time corrections for particle counters. Part II: High concentration measurements with an FSSP. *J. Atmos. Oceanic Technol.*, **6**, 585–598.

——, and L. Amodei, 1989: Coincidence and dead-time corrections for particle counters. Part I: A general mathematical formalism. *J. Atmos. Oceanic Technol.*, **6**, 575–584.

Cerni, T. A., 1983: Determination of the size and concentration of cloud drops with an FSSP. *J. Climate Appl. Meteor.*, **22**, 1346–1355.

Cooper, W. A., 1988: Effects of coincidence on measurements with a forward scattering spectrometer probe. *J. Atmos. Oceanic Technol.*, **5**, 823–832.

Dye, J. E., and D. Baumgardner, 1984: Evaluation of the forward scattering spectrometer probe: I: Electronic and optical studies. *J. Atmos. Oceanic Technol.*, **1**, 329–344.

Knollenberg, R. G., 1981: Techniques for probing cloud microstructure. *Clouds, Their Formation, Optical Properties, and Effects*, P. V. Hobbs, A. Deepak, Eds. Academic Press, 495 pp.

Markowski, G. R., 1987: Improving Twomey's algorithm for inversion of aerosol data. *Aerosol Sci. Technol.*, **7**, 127–141.

Pinnick, R. G., D. M. Garvey and L. D. Duncan, 1981: Calibration of Knollenberg FSSP light-scattering counters for measurement of cloud droplets. *J. Appl. Meteor.*, **20**, 1049–1057.

Wolfe, P., 1959: The secant method for simultaneous nonlinear equations. *Commun. Assoc. Comput. Mach.*, **2**, 12–13.